Tight-binding Study of Γ-L Bandstructure Engineering for Ballistic III-V nMOSFETs

Ze Yuan, Aneesh Nainani, Ximeng Guan, H. –S. Philip Wong and Krishna C. Saraswat
Center for Integrated Systems, Department of Electrical Engineering
Stanford University, Stanford, CA 94305, USA

Abstract— **A major concern for III-V nMOSFETs is the degradation of I_{ON} due to low density of states and spillover of the charge from high-mobility Γ-valley to low-mobility L-valley at high sheet charge density. In this paper, we study these Γ-L bandstructure effects for ultrathin-body $In_xGa_{1-x}Sb$ nMOSFETs with varying stoichiometry using tight-binding and ballistic transport model.**

Keywords- tight-binding, ballistic transport, ultra-thin body, InGaSb.

I. INTRODUCTION

nMOSFETs based on III-V materials have the highest mobility/injection velocity (v_{inj}), the major concern however, is the degradation of device performance due to low density-of-states (DOS) (low effective mass of carriers) and spillover of the charge from high-mobility Γ- to low-mobility L-valley at high sheet charge [1-3]. In this paper, we study these Γ-L bandstructure effects for varying stoichiometry of $In_XGa_{1-X}Sb$, which has high mobility for both electrons [4] & holes [5] and is a promising candidate for future technology nodes.

For performance evaluation of ultrathin-body (UTB) double-gate devices, the use of bulk effective masses is not adequate [6]. E-k relations for $In_XGa_{1-X}Sb$ UTB MOSFET (Fig. 1) are calculated using $sp^3d^5s^*$ atomistic tight-binding (TB) model coupled with Poisson's equation. The effect of varying the In % on DOS, electron population among Γ-, L-, and X-valleys is studied systematically. E-k band diagrams for UTB MOSFET with GaSb and InSb channel are plotted in Fig. 2. Amongst different valleys of electrons, Γ-valley has lower effective mass, thus higher v_{inj} but lower DOS. For GaSb and low In% $In_XGa_{1-X}Sb$, due to low energy separation between Γ- and L-valleys ($\Delta_{\Gamma\text{-}L}$), L-valley can also be populated, which has higher DOS but lower v_{inj}. Increasing In% in the compound brings up L-valley, reduces the energy for Γ-valley, meanwhile reducing the effective mass of Γ-valley. However, high In% makes it difficult to achieve high electron sheet charge density (N_S) from Γ-valley (due to the low DOS). For high drive current, high v_{inj} and N_S have to be achieved simultaneously, which requires engineering of DOS, v_{inj} and electrons population in different valleys. We study the effect of all these factors (Fig. 3): The band energy (Fig. 5) & difference in DOS (Fig. 6) among Γ- and L-valleys determines the overall population among different valleys (Fig. 7). Using N_S (Fig. 8) and v_{inj} (Fig. 9), ballistic drive current (Fig. 10) is calculated and compared for varying In %.

II. METHODOLOGY

TB parameters for ternary $In_XGa_{1-X}Sb$ are calculated following virtual-crystal approximation (VCA) incorporating compositional disorder effect and fitted to bulk band gap of ternary compound [7-8]. 1D Poisson's equation perpendicular to channel direction is coupled with TB Hamiltonian by Hartree-Fock potential in the gate stack. Dangling bonds at interface are pacified by hydrogen termination of hybridized orbitals to eliminate all the states within band gap [9]. A ballistic transport model is adopted to assess transport of electrons [10]. v_{inj} is determined from full band structure with non-parabolic E-k relationship considered for all valleys.

III. SIMULATION RESULTS

A. Band energy, DOS and Valley Population

Band structures of $In_XGa_{1-X}Sb$ for T_{BODY}=4nm at N_S of ~$3\times10^{12}cm^{-2}$ for different In %'s are compared in Fig. 4. For low In % $In_XGa_{1-X}Sb$, because of quantum confinement (QC) effects, $\Delta_{\Gamma\text{-}L}$ is marginal, especially under high V_G and thin T_{BODY}, resulting in Fermi level moving into L-valley. Band gap (E_g) & $\Delta_{\Gamma\text{-}L}$ are shown in Fig. 5: with higher In%, $\Delta_{\Gamma\text{-}L}$ is increased (from ~0 to ~0.7eV) to confine more electrons in Γ-valley counteracting the effects of quantization (Fig. 5(a)), which is more dominant for thin T_{BODY} (Fig. 5(b)) ($\Delta_{\Gamma\text{-}L}$ ~0.5eV for T_{BODY}=7nm, ~0.43eV for T_{BODY}=3nm, In % 0.5). At higher N_S (V_G), though E_g is lowered due to quantum confinement stark effect [11] (from ~0.5 to ~0.35eV for T_{BODY}=4nm, In % 0.5), $\Delta_{\Gamma\text{-}L}$ stays low (Fig. 5(c)) (~0.03eV for T_{BODY}=4nm, GaSb). This can be attributed to Γ-valley's curvature getting blunt (effective mass becomes larger) at high N_S, thus alleviated quantization effect. Fig. 6 plots the 2-D DOS, Γ-valley has 100x lower DOS compared with L-valley, which is required to achieve high N_S. In-rich compounds lead to decrease in DOS at conduction band edge (~10^{15} $eV^{-1}cm^{-2}$ GaSb, ~10^{13} $eV^{-1}cm^{-2}$ InSb) meaning further movement of Fermi level (read higher V_G) is necessary to achieve same N_S. % occupation of electrons in Γ-valley is plotted against In %, T_{BODY} and N_S in Fig. 7. From $\Delta_{\Gamma\text{-}L}$ for reasonable In %, adequate percentage of charge can be confined in Γ-valley (~100% at $1\times10^{11}cm^{-2}$ for In % 0.5) even at high N_S (~60% for $4\times10^{12}cm^{-2}$, In % 0.5) and thin T_{BODY} (~50% for T_{BODY}=3nm, In % 0.5). Fig. 8 illustrates (a) sheet charge density as a function of gate voltage and (b) sub-threshold swing comparison. Two slopes in N_S can be identified which correspond to Γ- and L-valleys respectively. For higher In

978-1-61284-418-3/11/$26.00

composition, loss in DOS at band edge requires much higher gate voltage to obtain sheet charge density of reasonable level for device operation (to get $2\times10^{12}cm^{-2}$ GaSb ~0.4V, InSb ~1.3V). The change in DOS as well as dielectric constant (from 14.4 GaSb to 16.8 InSb) is also reflected in the degradation of sub-threshold swing with increasing In % (100mV/dec for GaSb, 115mV/dec for InSb, T_{BODY} =4nm). For device geometry of interest, DOS determined quantum capacitance has an evident impact on the subthreshold behavior as subthreshold swing improves for larger T_{BODY} (95mV/dec for T_{BODY} =4nm, 100mV/dec for T_{BODY} =3nm, GaSb).

B. v_{inj}

I_{dsat}-V_G is evaluated by integrating N_S with average velocity of electrons along transport direction at each k point. Parasitic resistance is neglected in the calculation. <100> is set as the transport direction. The average velocity at given gate bias can be calculated by taking the ratio between the overall current density and sheet charge density [10]. Under the ballistic transport model, when Fermi level is below conduction band edge, the injection velocity stays constant; it increases as Fermi level moves into conduction band. As shown in Fig. 9, since electron population is mostly in L-valley, the overall v_{inj} of GaSb and Ga-rich $In_XGa_{1-X}Sb$ is low (~2×10^7cm/s) at high N_S as most of the electrons are in L-valley. In-rich compounds give high v_{inj} (~1×10^8cm/s), because of sharper curvature of Γ-valley in calculated E-k relation, however population of L-valley leads to the decrease in v_{inj} at high N_S (~$10^{12}cm^{-2}$ for In % 0.5). By engineering with $\Delta_{\Gamma\text{-}L}$ and DOS for the optimal driving capability, the overall v_{inj} can maintain high (~1×10^8cm/s) with adequate % of charge in Γ-valley, when DOS of L-valley starts to contribute to N_S.

C. Performance Evaluation

In Fig. 8 (a), the filling of L-valley gives raise in N_S. Without excessive filling of L-valley, average injection velocity maintains high as shown in Fig. 9. Fig. 10 shows proper amount of In percentage (~25%) in $In_XGa_{1-X}Sb$ can give a overall improvement in drive-current by maintaining high v_{inj} with sufficient amount of charge in Γ-valley. Further increase in In composition leads to significant loss in N_S. Drive current for $In_{0.25}Ga_{0.75}Sb$ is 50% higher than silicon, 30% higher than GaSb (highest DOS) and 120% higher than InSb (highest v_{inj}) at an over-drive voltage of 0.7V. It is shown that varying stoichiometry of III-V compound material allows careful engineering of Γ-L band structure, to achieve optimal trade-off between v_{inj} and DOS.

IV. CONCLUSION

Γ-L bandstructure effects in ultra-thin body III-V nMOSFETs are studied using tight-binding and ballistic transport model. It is shown by varying In % in $In_XGa_{1-X}Sb$, most of electrons can be kept in the Γ-valley at relevant N_S values to avoid excessive population of electrons in the L-valley (GaSb) or significant loss of charge due to low DOS (InSb), hence achieves the best I_{DSAT} .

ACKNOWLEDGMENT

One of the authors (Ze Yuan) would like to thank Stanford Graduate Fellowship for the financial support.

REFERENCES

[1] S. Takagi, T. Irisawa, T. Tezuka, T. Numata, S. Nakaharai, N. Hirashita, Y. Moriyama, K. Usuda, E. Toyoda, S. Dissanayake, M. Shichijo, R. Nakane, S. Sugahara, M. Takenaka, N. Sugiyama, "Carrier-transport-enhanced channel CMOS for improved power consumption and performance," Electron Devices, IEEE Transactions on, vol. 55, p. 21, Jan. 2008.

[2] A. Rahman, G. Klimeck, M. S. Lundstrom, "Novel channel materials for ballistic nanoscale MOSFETs-bandstructure effects," IEDM Technical Digest, Dec. 2005, p. 604.

[3] M. Rodwell, W. Frensley, S. Steiger, E. Chagarov, S. Lee, H. Ryu, Y. Tan, G. Hegde, L. Wang, J. Law, T. Boykin, G. Klimeck, P. Asbeck, A. Kummel, J. N. Schulman, "III-V FET channel designs for high current densities and thin inversion layers," Device Research Conference, p. 149, Jun. 2010.

[4] B. R. Bennett, R. Magno, J. B. Boos, W. Kruppa, M. G. Ancona, "Antimonide-based compound semiconductors for electronic devices: A review," Solid-State Electronics, vol. 49, p. 1875, Dec. 2005.

[5] A. Nainani, T. Irisawa, Z. Yuan, Y. Sun, T. Krishnamohan, M. Reason, B. R. Bennett, J. B. Boos, M. G. Ancona, Y. Nishi, K. C. Saraswat, "Development of high-k dielectric for antimonides and a sub 350°C III-V pMOSFET outperformaning Germanium," IEDM Technical Digest, Dec. 2010, p. 138.

[6] L. Yang, N. Neophytou, T. Low, G. Klimeck, M. S. Lundstrom, "A tight-binding study of the ballistic injection velocity for ultrathin-body SOI MOSFETs," Electron Devices, IEEE Transactions on, vol. 55, p. 866, Mar. 2008.

[7] J.-M. Jancu, R. Scholz, F. Beltram, F. Bassani, "Empirical spds* tight-binding calculation for cubic semiconductors: General method and material parameters," Physical Review B, vol. 57, p. 6493, Mar. 1998.

[8] S. J. Lee, H. S. Chung, K. Nahm, C. K. Kim, "Band structure of ternary-compound semiconductors using a modified tight-binding method," Physical Review B, vol. 42, p. 1452, Jul. 1990.

[9] S. Lee, F. Oyafuso, P. von Allmen, G. Klimeck, "Boundary conditions for the electronic structure of finite-extent embedded semiconductor nanostructures," Physical Review B, vol. 69, 045216, Jan. 2004.

[10] A. Rahman, G. Jing, S. Datta, M. S. Lundstrom, "Theory of ballistic nanotransistors," Electron Devices, IEEE Transactions on, vol. 50, p. 1853, Sept. 2003.

[11] X. Guan, Y. Tan, J. Lu, Y. Wang, Z. Yu, "A self-consistent simulation of InSb double-gate MOSFETs using full-band tight-binding approach," International Conference on Simulation of Semiconductor Processes and Devices, p. 161, Sept. 2007.

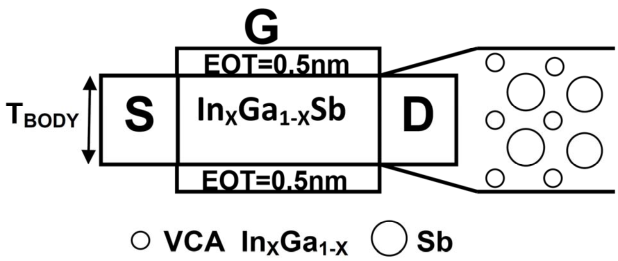

Figure 1. Structure of $In_XGa_{1-X}Sb$ double-gate MOSFET with (100) orientation. Atom arrangement under VCA

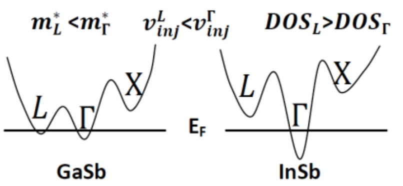

Figure 2. Band diagrams of GaSb and InSb.

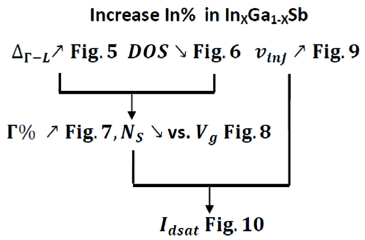

Figure 3. Bandstructure effects by varying In% in $In_XGa_{1-X}Sb$ and their relationships. Effects studied are plotted in corresponding figures.

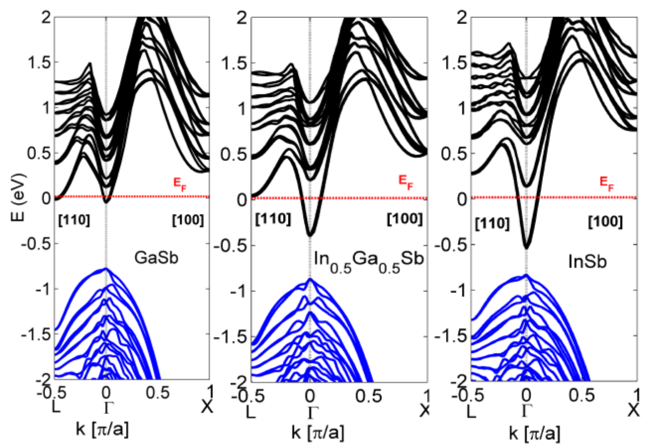

Figure 4. Calculated band structure from TB for $In_XGa_{1-X}Sb$ at sheet charge density ~ $3\times10^{12}cm^{-2}$ with a body thickness of 4nm.

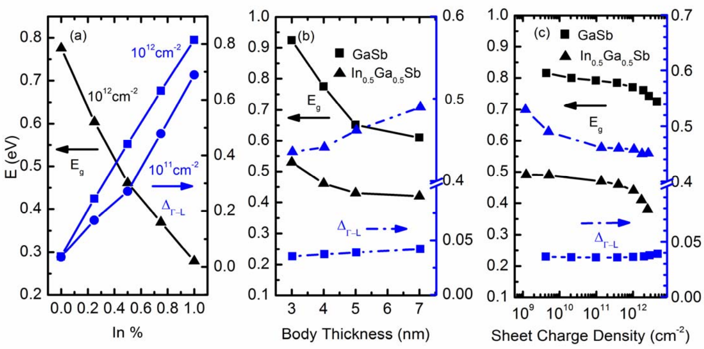

Figure 5. Calculated band gap and Γ-L energy separation vs. (a) In composition for 4nm body thickness and ~ 10^{11} &$10^{12}cm^{-2}$ sheet charge density; (b) body thickness for sheet charge density ~ $1\times10^{12}cm^{-2}$; (c) sheet charge density for 4nm body thickness.

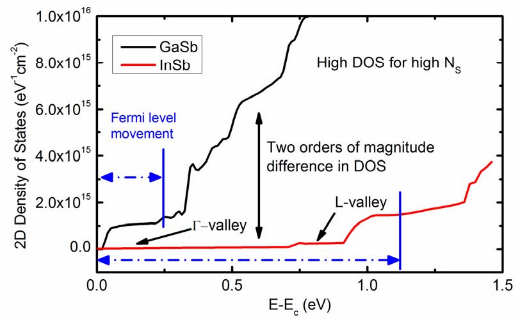

Figure 6. 2D Density of States for GaSb and InSb for body thickness of 4nm.

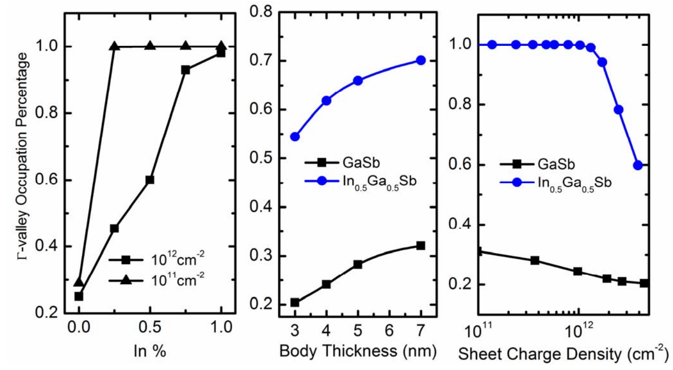

Figure 7. Percentage of electron occupation in Γ-valley vs. (a) In composition for 4nm body thickness and ~ $10^{11}cm^{-2}$ & $10^{12}cm^{-2}$ sheet charge density; (b) body thickness for ~$1\times10^{12}cm^{-2}$ sheet charge density; (c) sheet charge density for 4nm body thickness.

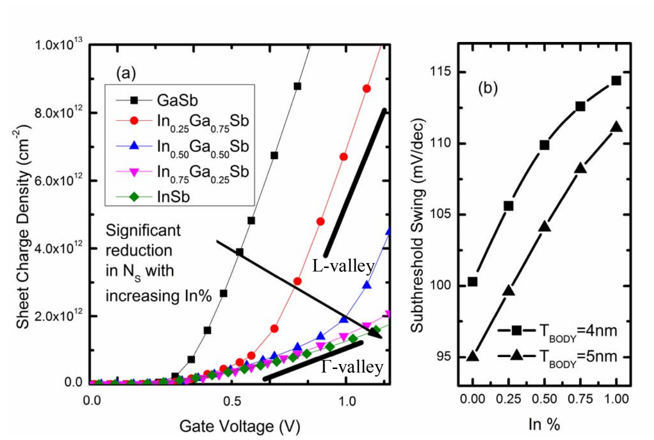

Figure 8. (a) sheet charge density as a function of gate voltage. Gate voltage is adjusted to give $5\times10^7cm^{-2}$ sheet charge at 0V; (b) subthreshold swing with varying In composition for body thickness of 4nm & 5nm.

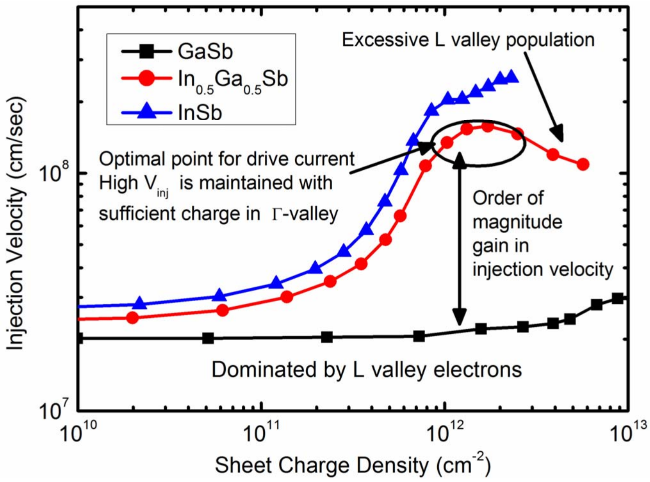

Figure 9. Injection velocity as a function of sheet charge density for different In composition, the drop in injection velocity at high sheet charge is due to L-valley population.

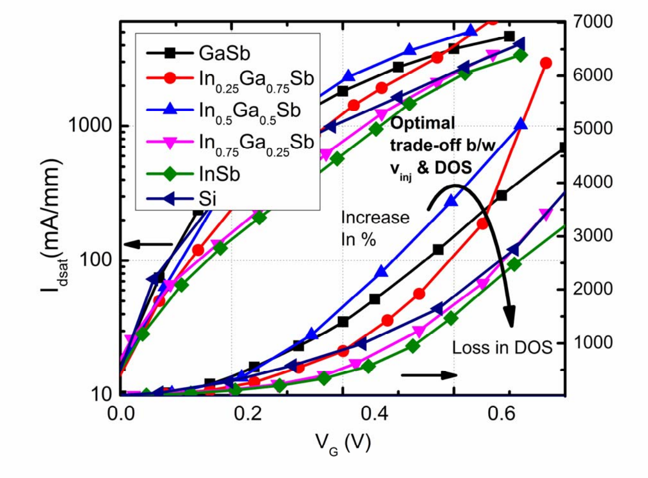

Figure 10. Saturation current as a function of gate voltage; Gate voltage is adjusted to give 15μA/μm current density at 0V.